Hindawi Publishing Corporation
EURASIP Journal on Wireless Communications and Networking
Volume 2008, Article ID 540873, 14 pages
doi:10.1155/2008/540873

Research Article

MACD-Based Motion Detection Approach in Heterogeneous Networks

Yung-Mu Chen, Tein-Yaw Chung, Ming-Yen Lai, and Chih-Hung Hsu

Department of Computer Science and Engineering, Yuan Ze University, 135 Yuan-Tung Road, Chung-Li, Taiwan 32003, Taiwan

Correspondence should be addressed to Tein-Yaw Chung, csdchung@saturn.yzu.edu.tw

Received 2 January 2008; Revised 19 May 2008; Accepted 22 July 2008

Recommended by Athanasios Vasilakos

Optimizing the balance between handoff quality and power consumption is a great challenge for seamless mobile communications in wireless networks. Traditional proactive schemes continuously monitor available access networks and exercise handoff. Although such schemes achieve good handoff quality, they consume much power because all interfaces must remain on all the time. To save power, the reactive schemes use fixed RSS thresholds to determine when to search for a new available access network. However, since they do not consider user motion, these approaches require that all interfaces be turned on even when a user is stationary, and they tend initiate excessive unnecessary handoffs. To address this problem, this research presents a novel motion-aware scheme called network discovery with motion detection (NDMD) to improve handoff quality and minimize power consumption. The NDMD first applies a moving average convergence divergence (MACD) scheme to analyze received signal strength (RSS) samples of the current active interface. These results are then used to estimate user's motion. The proposed NDMD scheme adds very little computing overhead to a mobile terminal (MT) and can be easily incorporated into existing schemes. The simulation results in this study showed that NDMD can quickly track user motion state without a positioning system and perform network discovery rapidly enough to achieve a much lower handoff-dropping rate with less power consumption.

1. INTRODUCTION

As wireless technologies advance, various wireless networks such as UMTS, WiFi, and WiMax networks are expected to jointly support universal ubiquitous services for future mobile users. To enjoy such ubiquitous services, equipping a mobile terminal (MT) with multiple network interfaces (or multimode) is getting more important. To ensure ubiquitous access, a multimode MT must seamlessly switch, or handoff, its connection between access points or base stations as users move between wireless networks.

Maintaining good handoff quality with minimal power consumption is an essential capability of multimode MT [1–3]. An active interface in a regular single-mode MT continuously monitors available access points and executes handoff whenever it is beneficial in a homogeneous wireless network. However, the scenario for multimode handsets differs. To continuously monitor varying wireless networks, a multimode MT must always turn on all other interfaces not currently in use. Although this proactive scheme ensures seamless handoff, a multimode MT requires much more power than a single-mode MT.

To reduce power consumption, a multimode MT uses existing reactive schemes [4–7] that turn on all interfaces for network discovery only when the RSS or frame error rate (FER) of the current active interface exceeds a predetermined threshold. These reactive schemes, however, are insufficiently reliable for handoff when users are quickly moving away from an access point (AP) or a base station (BS), and they often activate interfaces unnecessarily even when users are stationary. Therefore, activating interfaces for network discovery according to user motion is important for improving handoff quality and minimizing power requirements.

This work presents a novel motion-aware scheme, called network discovery with motion detection (NDMD) to assist a handset in improving its handoff quality while reducing power consumption. In NDMD, when a user moves away from AP, an MT must start discovering available networks in its neighborhood early to avoid handoff failure. On the other hand, an MT can stop network discovery when a user is stationary even if the user is far from the BS or AP. Thus, NDMD can reduce the handoff dropping rate and power consumption of an MT.

The proposed NDMD system employs a user motion detection (UMD) mechanism to estimate the user motion state. The UMD analyzes RSS samples from current active interface then applies a moving average convergence divergence (MACD) scheme [8] to determine the user motion state. The MACD consists of two lowpass filters with different smoothing factors. Since accurately estimating user motion requires accurately selecting smoothing factors, this study presented a set of possible choices and evaluated their respective performance. In contrast with previous work [7, 9–12] that exploit a positioning system to maintain handoff quality, UMD estimates user motion states by analyzing RSS samples. Therefore, no additional hardware, such as GPS, is needed.

The NDMD has advantages as follows. (1) Without a positioning system, the MT can determine whether the user is leaving the AP, approaching the AP or stationary. (2) An MT can activate and terminate its interfaces rapidly enough to minimize the handoff dropping rate and power consumption. (3) The simplicity of the system requires minimal computing overhead. (4) Because the NDMD can initiate network discovery, it can be combined with all handoff decision mechanisms.

The rest of this paper is organized as follows. Section 2 discusses related network discovery mechanisms. Section 3 presents details of the predictive algorithm for network discovery. Section 4 evaluates the performance of NDMD. Finally, Section 5 draws conclusions and discusses future works.

2. RELATED WORK

Current network discovery mechanisms can be categorized as proactive, reactive [13], and location-aware [14]. A common proactive approach uses a decision function based on a handoff mechanism. In a heterogeneous network environment, traditional RSS comparisons [15, 16] are unreliable for or incapable of making accurate handoff decisions. Therefore, many metrics, such as service type, monetary cost, network conditions, user preferences, velocity, have been adopted in decision functions [17–20] to determine whether a handoff is needed. In the proactive approach, an MT must turn on all its interfaces to perform network discovery in advance and then monitor all available networks. These approaches can reduce handoff latency, but it substantially increases power consumption. Although Al-Gizawi et al. [20] proposed a mechanism for periodic, on demand or by event network discovery in a UMTS-WLAN interoperability platform, their methods were not described in detail.

On the other hand, many researchers have studied reactive network discovery schemes [4–7] that trigger handoff initiation by using predefined thresholds. However, few have addressed the problem of network discovery. Power consumption and handoff dropping rate are a tradeoff if a predefined RSS threshold is adopted for network discovery. For instance, if the RSS threshold is high, power consumption may increase as an MT turns on its interfaces early for network discovery, which then enhances handoff. In contrary, if the RSS threshold is set to a low value, the handoff dropping rate may increase if the MT may turn on its interfaces late and leaves insufficient time for the MT to perform network discovery and handoff execution.

In location-aware schemes [7, 9–12], location information services such as GPS, location service server (LSS), and topology map are used to provide information such as coverage area, latency, and bandwidth of available wireless networks around an MT. In [7, 12], an MT first determines whether the RSS falls below a predefined RSS threshold. If so, the MT applies a decision function to determine whether handoff is required based on the information that provided by LSS. If a handoff is not required, the MT does not activate other interfaces to save battery power. However, this work demonstrates only the results of MT energy consumption but does not evaluate the handoff dropping rate.

In [10], a handoff trigger node installed in a WLAN/cellular transition region to generate a specific link layer trigger for vertical handoff. This specific trigger can enable an MT to initiate the vertical handoff process in time to reduce the handoff latency and the handoff dropping rate. However, the authors did not describe the details of interface management. In an earlier work [9], the authors assumed that an MT manages its WLAN interface using a location-aware base station controller (BSC). Based on BSC, an MT can activate or terminate the WLAN interface in an appropriate time to reduce power consumption. However, a reactive method was also used for handoff initiation.

In [11], a positioning system and LSS were employed for network discovery to reduce unnecessary power consumption during handoff. Based on the distance between an AP and an MT, the MT uses various time intervals to perform network discovery. If the distance to the AP is long, then the MT requires a long time interval to perform network discovery. However, the LSS-based network discovery scheme requires additional hardware and cannot be implemented in an indoor environment where no positioning system can work.

3. NETWORK DISCOVERY WITH MOTION DETECTION

An MT must detect the movement of users to predict when they leave or enter the associated AP. The user behavior can be classified into the following three states: (1) approaching state: the user is moving toward the AP; (2) leaving state: the user is leaving the AP; (3) stationary state: the user is stationary. By using a user motion detection (UMD), an MT can easily apply RSS to identify the user state without the assistance of a positioning system.

The simplest method for detecting the user motion state is RSS. Since the receiving signal power of an MT is related to the distance between the MT and its associated AP, the received signal power P_r at distance d is given by

$$P_r[i] = P_t - 10\rho \log[d] + X_{dB}, \tag{1}$$

where i is an accumulated value that is determined by the measuring frequency, P_t is the transmitted signal power,

ρ is the path loss exponent, and X_{dB} is a Gaussian random variable with zero mean and standard deviation σ_{dB} (also called shadowing deviation) representing shadow fading. According to (1), the difference between two consecutive measured received signal powers at distances d_1 and d_2 can, without considering X_{dB}, be expressed as

$$\Delta P_r[i] = P_r[i] - P_r[i-1] = -10\rho \log\left[\frac{d_2}{d_1}\right]. \quad (2)$$

Given the measured RSS interval and the direction and speed of user motion, the following characteristics of mobile radio propagation can be specified based on (2). UMD motion behavior

$$(\text{DIF}) = \begin{cases} \text{Stationary state}, & \text{if } d_1 = d_2,\ \Delta P_r = 0, \\ \text{Approaching state}, & \text{if } d_1 > d_2,\ \Delta P_r > 0, \\ \text{Leaving state}, & \text{if } d_1 < d_2,\ \Delta P_r < 0. \end{cases} \quad (3)$$

Thus, the variation in ΔP_r indicates the motion state of a user. However, the received signal power measured by an MT fluctuates constantly because of the fading effect even if a user is in a stationary state. Therefore, an MT cannot easily detect user motion based only on the difference between two consecutive RSS values.

3.1. MACD-based UMD mechanism

This work uses a trend-following indicator called moving average convergence divergence (MACD) [8] to elucidate a user behavior in a wireless environment without a positioning system. The MACD involves two exponentially weighted moving average (EWMA) filters to analyze the time series data. These two EWMA filters can be expressed as follows:

$$E[i] = (1-\alpha)E[i-1] + \alpha O[i], \quad (4)$$

where $E[i]$ is the current estimate of the time series data, $E[i-1]$ is the prior estimate, $O[i]$ is the current observation, and α is a smoothing factor within the range zero to one. Equation (4) indicates that $E[i]$ represents a compromise between a previous estimate and the current observation. If α is large, then the current observation is emphasized, and the filter provides good agility. That is, the estimate can be generated rapidly in response to changes in time series data. If α is small, more emphasis is given to the prior estimate, and the filter provides good stability. Restated, the generated estimate can resist the noise in individual observations but cannot react rapidly to changes in time series data. Therefore, the EWMA filter can provide different reactivity with different α.

The MACD employs two EWMA filters to calculate an agile estimate and a stable estimate in a single time series data. If the observed values are increasing constantly, then the rising velocity of the agile estimate exceeds that of the stable estimate. Restated, the difference between the agile estimate and the stable estimate increases. This phenomenon is called divergence. Similarly, if the observed values decline constantly, the same phenomenon occurs. If the observed values remain constant, the agile estimate and the stable estimate gradually converge toward the same value. That is, the difference between the agile estimate and stable estimate becomes smaller. This phenomenon is called convergence. Based on the difference between the agile estimate and the stable estimate, MACD can reduce random fluctuations and identify the underlying direction (upward, downward, or unchanging) in the time series data. Since RSS is also time series data and changes with user motion, UMD uses MACD to smooth RSS fluctuation and identify RSS changes. The MT can then determine the user motion state.

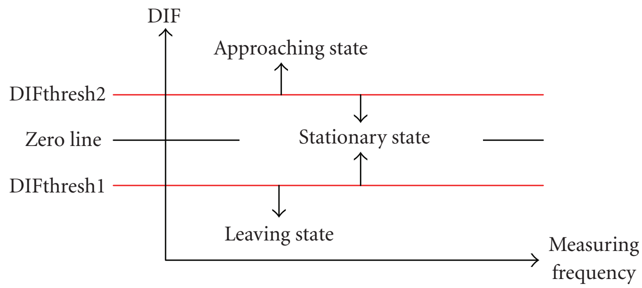

Figure 1: Determining user's behavior.

The proposed UMD mechanism operates as follows. It first adopts EWMA filter in MACD to calculate two smoothed received signal strengths (SRSSs). Let α and β be the smoothing factors used to calculate the agile and stable SRSS, respectively. $R[i]$ is the received signal strength measured by an MT. According to (4), the agile SRSS $A[i]$ and stable SRSS $S[i]$ can be obtained by

$$\begin{aligned} A[i] &= (1-\alpha)A[i-1] + \alpha R[i], \\ S[i] &= (1-\beta)S[i-1] + \beta R[i], \end{aligned} \quad (5)$$

where the initial values of $A[0]$ and $S[0]$ equal $R[0]$. Since β must be smaller than α, the following relationship is defined:

$$0 < \beta < \alpha < 1, \quad \beta = \frac{\alpha}{k},\ k > 1, \quad (6)$$

where k is a constant value. The difference DIF between the agile SRSS $A[i]$ and the stable SRSS $S[i]$ is defined as follows:

$$\text{DIF}[i] = A[i] - S[i]. \quad (7)$$

The DIF can determine user state. As **Figure 1** shows, two DIF thresholds are defined to determine user behavior. Based on the DIF value and the DIF thresholds, the detection of user motion state by ΔP_r is modified as follows: UMD motion behavior

$$(\text{DIF}) = \begin{cases} \text{Stationary}, & \text{if DIFthresh2} > \text{DIF} > \text{DIFthresh1}, \\ \text{Approaching}, & \text{if DIF} > 0,\ \text{DIF} > \text{DIFthresh2}, \\ \text{Leaving}, & \text{if DIF} < 0,\ \text{DIF} < \text{DIFthresh1}. \end{cases} \quad (8)$$

3.2. NDMD algorithm

Based on the user motion state determined by UMD, NDMD activates or terminates an MT interfaces for network

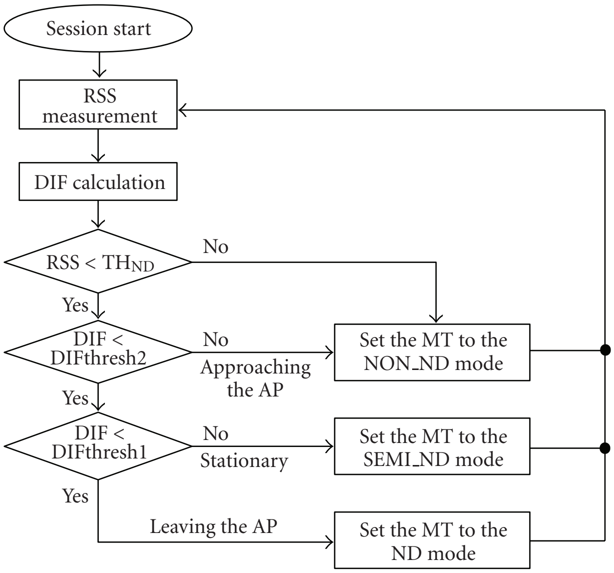

Figure 2: The NDMD algorithm for network discovery.

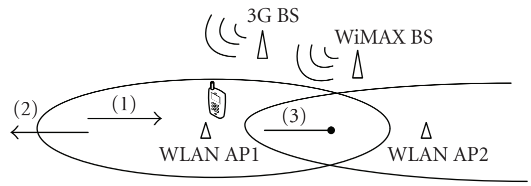

Figure 3: Example of proposed algorithm.

discovery at the right time to save power and reduce handoff dropping rate. In NDMD, a new network discovery threshold (TH_{ND}) and three network discovery modes are defined. The higher TH_{ND} is necessary since an MT must turn on all its interfaces in time to perform network discovery procedures such as searching base stations, association, AAA, address acquisition, and other high layer signaling functions, before switching to another network. However, using a high RSS threshold certainly increases power consumption. Therefore, the following three network discovery modes are defined to reduce power consumption.

(i) NON_ND mode: this mode is used when a user is approaching an AP or BS. Therefore, network discovery is unneeded.

(ii) ND mode: this mode is used when a user is leaving the associated AP or BS. Therefore, timely activation of interfaces is critical for detecting all available wireless networks.

(iii) SEMI_ND mode: this mode is applied when a user is stationary. An MT first determines whether any APs or BSs is available in its neighborhood. If so, it determines whether a horizontal handoff is required. Otherwise, the MT must activate all of its interfaces to perform network discovery.

Figure 2 shows a flow chart of the NDMD algorithm. When an MT connects to an AP, the RSS is measured and the user motion is continuously determined. When the RSS is below or above the predefined RSS threshold mentioned above, the MT is set to change to a suitable network discovery mode to activate or terminate its interfaces based on the NDMD algorithm.

Figure 3 presents an example of NDMD application. Suppose an MT is currently associated with WLAN AP1. In scenario (1), the MT can terminate its network discovery even if its initial location is far from AP1, because the user is in an approaching state. In scenario (2), the MT activates its interfaces to discover other networks in time to reduce the handoff dropping rate because it is leaving the associated AP. In scenario (3), the user is leaving AP1 initially but stops before he has left. In this case, the MT certainly activates all its interfaces to discover other available networks when the RSS of the MT is below the predefined network discovery threshold. However, the proposed algorithm eventually detects that the user is in a stationary state, thus the MT turn off other interfaces to reduce power consumption. Here, the MT simply determines whether a horizontal handoff is required because AP2 is nearby.

3.3. *Analysis of NDMD algorithm*

In NDMD, an MT can predict whether a user is leaving its associated WLAN by applying UMD and then activating or terminating its interfaces within an appropriate time. The UMD strongly affects the performance of the NDMD algorithm. The change of DIF is used to determine the motion state of a user in UMD. Thus, the DIF value must respond quickly to user behavior so that the motion state can be determined rapidly. The analysis requires determining the difference, δ DIF, between two consecutive DIF values.

Substituting (5) into (7) yields

$$\begin{aligned}\mathrm{DIF}[i] &= A[i-1] - S[i-1] + \alpha(R[i] - A[i-1]) \\ &\quad - \beta(R[i] - S[i-1]) \\ &= \mathrm{DIF}[i-1] + \alpha(R[i] - A[i-1]) \\ &\quad - \beta(R[i] - S[i-1]).\end{aligned} \tag{9}$$

Let ΔDIF denotes DIF[i] − DIF[$i-1$], the DIF is given by

$$\Delta\mathrm{DIF}[i] = \alpha(R[i] - A[i-1]) - \beta(R[i] - S[i-1]). \tag{10}$$

Using $\beta = \alpha/k$ in (6), we have

$$\Delta\mathrm{DIF}[i] = \alpha\left[(R[i] - A[i-1]) - \frac{1}{k}(R[i] - S[i-1])\right]. \tag{11}$$

Equation (11) shows that α, k, $(R[i] - A[i-1])$, and $(R[i] - S[i-1])$ strongly affect ΔDIF. $(R[i] - A[i-1])$ and $(R[i] - S[i-1])$ represent two forms of ΔDIF, which are the differences between two consecutive RSS measurements.

The ΔDIF is affected by many other factors, such as mobile radio propagation characteristics. Some of these factors are summarized as follows.

(i) *Smoothing factor* α*:* according to (11), if k, $(R[i] - A[i-1])$ and $(R[i] - S[i-1])$ are fixed, the increasing α increases ΔDIF. However, since $A[i-1]$ and $S[i-1]$ are also governed by α, the effect of α must be discussed in detail here. Figure 4 presents the effect of the smoothing factor α on SRSS when the distance to the transmitter is large by using a computer simulation. The simulation result was produced by NS2 with a log normal shadow model. Here, SRSS represents either an agile SRSS or a stable SRSS. Consider the agile SRSS as an example. When α is set to one, SRSS is the actual RSS. The value of $(R[i] - A[i-1])$ with the larger α (dotted line) is smaller than that with a smaller α (dashed line). As the distance between the MT and the transmitter increases, the gap $(R[i] - S[i-1])$ with a large α (dotted line) decreases faster than a gap with a small α (dashed line). Therefore, although a large α can produce a large ΔDIF, ΔDIF decreases more rapidly than when α is small as the distance to the transmitter increases. Assume that SRSS with $\alpha = 0.5$ represents an agile SRSS, and SRSS with $\alpha = 0.1$ denotes a stable SRSS. As the distance between the transmitter and the MT increases, Figure 4 shows that the $(R[i] - S[i-1])$ gap remains very large although $(R[i] - A[i-1])$ gap becomes small. Moreover, ΔDIF bounces back because $(R[i]-A[i-1])$ may be less than $1/k(R[i]-S[i-1])$ when a user moves away from the transmitter beyond a particular distance.

(ii) *k value:* according to (11), given that α, $(R[i] - A[i-1])$ and $(R[i]-S[i-1])$ are fixed, a larger k can increase ΔDIF.

(iii) *Path loss:* path loss is the attenuation of an electromagnetic wave moving from a transmitter to a receiver and is governed by many factors, including carrier frequency, environmental factors (e.g., urban versus rural), distance between transmitter and receiver, and antennas height and others. According to (2), a larger (smaller) path loss exponent (ρ) implies larger (smaller) attenuation and ΔP_r. Restated, a larger (smaller) path loss corresponds to a larger (smaller) ΔDIF.

(iv) *Distance:* suppose that a user is leaving (approaching) a transmitter at a fixed speed, direction, and RSS measurement interval. According to (2), a longer (shorter) distance to the transmitter corresponds to a smaller (larger) d_2/d_1. Therefore, a longer (shorter) distance corresponds to a smaller (larger) ΔP_r or a smaller (larger) ΔDIF.

(v) *Velocity:* the following equation can be derived from (2),

$$\Delta P_r[i] = -10\rho \log\left[\frac{d_2}{d_1}\right] = -10\rho \log\left[\frac{d_1 + vt}{d_1}\right]. \quad (12)$$

Suppose a user is moving in a fixed direction. A larger velocity corresponds to a larger ΔP_r.

(vi) *Network type:* when a user moves with a fixed speed, direction, and RSS measurement interval, the ΔP_r measured in WiMAX or 3G is smaller than that measured in WLAN because the coverage of the former networks is larger.

3.4. Selection of UMD parameters

In the UMD, α and k must maintain DIF between DIFthresh1 and DIFthresh2 when a user is stationary and the RSS fluctuation of an MT varies due to fading effects. Therefore,

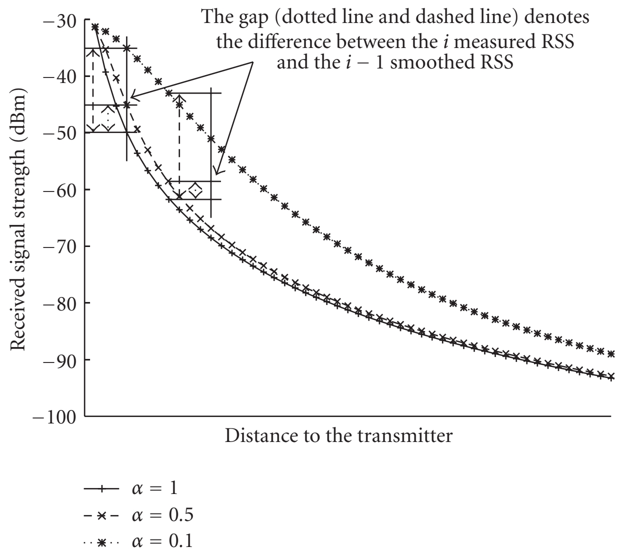

Figure 4: Effect of smoothing factor α.

choosing appropriate α and k is important for UMD to work well. Figure 5 plots the relationship among α, k, and the number of detected motions under various shadowing deviations (log normal shadow model) when a user is stationary. Accurate selection of α and k values minimizes the number of incorrect movement detections. Therefore, with reference to Figure 5, α and k should be chosen such that the number of motion detections approximates zero. Figures 5(a) and 5(b) also reveal that a larger shadowing deviation increases the number of detected motions.

According to the earlier analysis, maximizing α and k can increase ΔDIF to enable rapid detection of user state. However, Figure 5 also illustrates the inverse relationship between α and k. A large α can produce a large ΔDIF but ΔDIF quickly diminishes as a user moves away from an AP. Therefore, when an MT accesses a network with smaller coverage, such as a WLAN, it must use a large α and a small k to quickly determine the user motion state. However, when a user is in networks with large coverage such as 3G or WiMAX, the MT should use a small α and a large k so it can identify user motion even when the ΔP_r measured by the MT is very small and the user is moving at a low velocity.

4. PERFORMANCE EVALUATION

In this section, extensive simulations were conducted to evaluate the performance of UMD and NDMD. The ns-2 simulator [21] and the BonnMotion node-movement generation tool [22] were used for computer simulations. In all simulations, a log normal shadowing model was used to simulate the wireless environment. A simple straight movement trajectory and random waypoint mobility model were adopted to simulate a user movement trajectory. Figure 6 shows an example of the random waypoint mobility model and Figure 7 shows the example of straight movement trajectory. A single user with an MT in a single wireless environment is simulated.

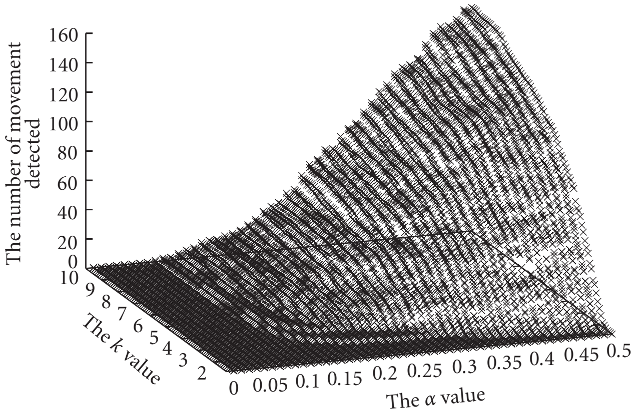

(a) Shadowing deviation = 4.0

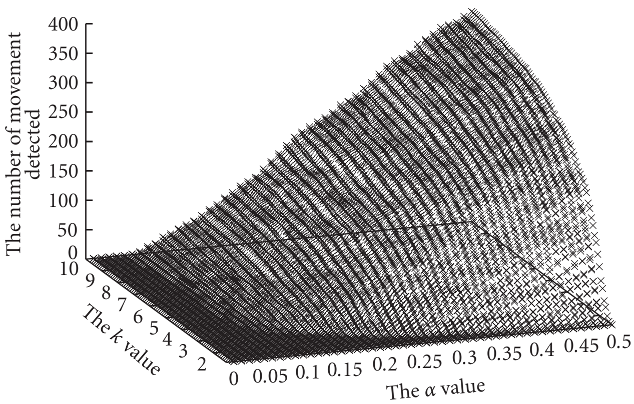

(b) Shadowing deviation = 6.0

Figure 5: Relationship among α, k, and number of detected motions (DIFthresh1 = −1, DIFthresh2 = 1, Sample Number = 1000).

4.1. *Evaluation of UMD mechanism*

The proposed UMD mechanism was evaluated by different α, k, shadowing deviation, velocity, and distance from an AP in a WLAN and a WMAN environment. In the WLAN environment, an MT equipped with an Orinoco 802.11 PC card in a closed environment [23] was simulated. In the WMAN environment, a customer premises equipment (CPE) was simulated based on information provided by the Airspan Corporation [24]. Table 1 shows the related parameters set to simulate the WLAN and WMAN environments.

4.1.1. *Comprehensive analysis*

As shown in Figure 7, a user is moving from location A to location C at 1 m/sec in a WLAN environment. Figure 8 shows the effect of using different α with fixed k on DIF value; the x-axis represents the distance between the MT and the transmitter. The negative x-axis represents the MT is approaching the transmitter and the positive x-axis represents the MT is leaving the transmitter. The results reveal that α barely affects the DIF value as a user approaches the transmitter. However, increasing α can rapidly reduce DIF when the user moves away from the transmitter. That is, the MT can rapidly detect the user's leaving state when a larger α is used in UMD.

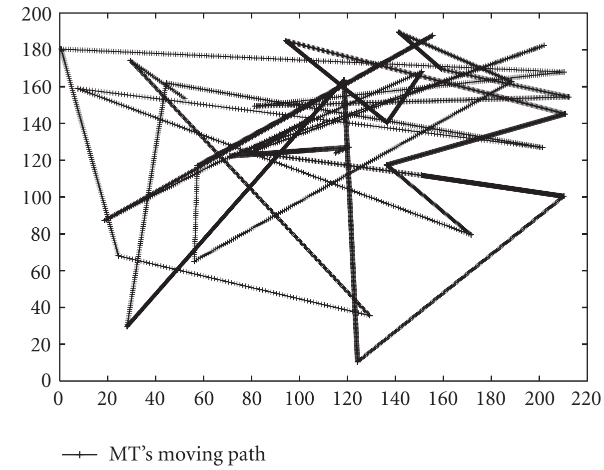

Figure 6: Examples of the random waypoint.

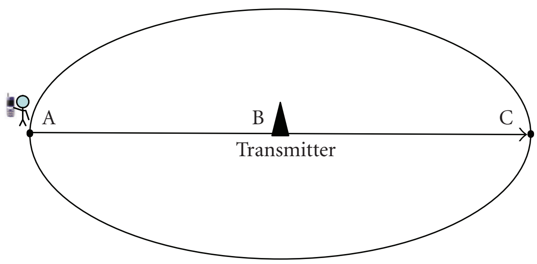

Figure 7: Examples of straight movement trajectory.

Table 1: Default parameters for the simulation of UMD mechanism.

Parameters for radio propagation		
Wireless environment	WLAN	WMAN
Cell radius (m)	50	740
Frequency (Hz)	2.472e9	3.5e9
Path loss exponent	4.0	3.0
Shadowing deviation (dB)	4.0	4.0
Transmitter antenna height (m)	1	40
Receiver antenna height (m)	1	2
Tx power (dBm)	15	27
Transmitter antenna gain (dB)	1	5
Receiver antenna gain (dB)	1	1
Rx sensitivity (dBm)	−94	−98
Parameters for mobile terminal		
Sampling interval (second)	0.1	0.5
Sampling size	8	4

Figure 9 presents the effect of using various k with a fixed α on the DIF value. The simulation results reveal that increasing k increases ΔDIF. Restated, increasing k enables faster and more accurate detection of user state. These two figures also show that, due to the effects of mobile radio

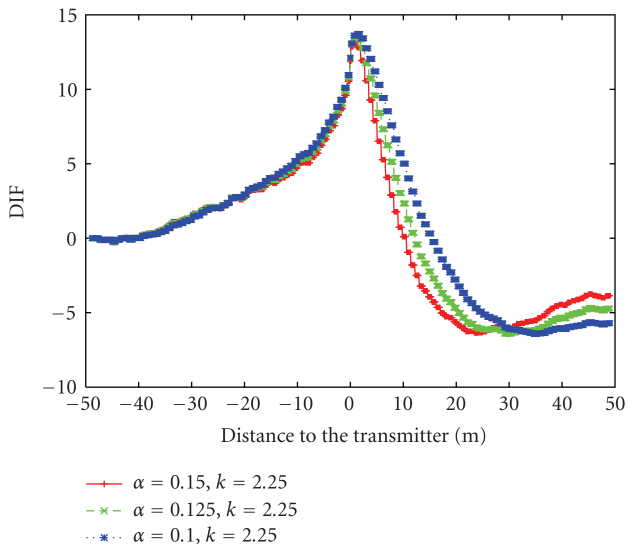

Figure 8: Effect of α in WLAN.

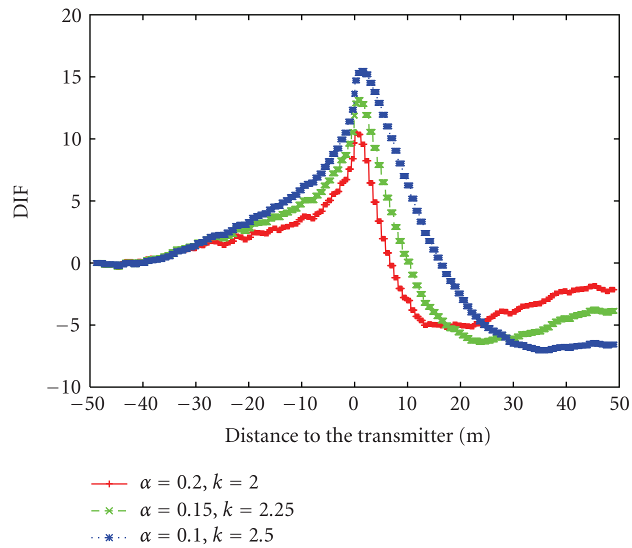

Figure 10: Effect of α and k in WLAN.

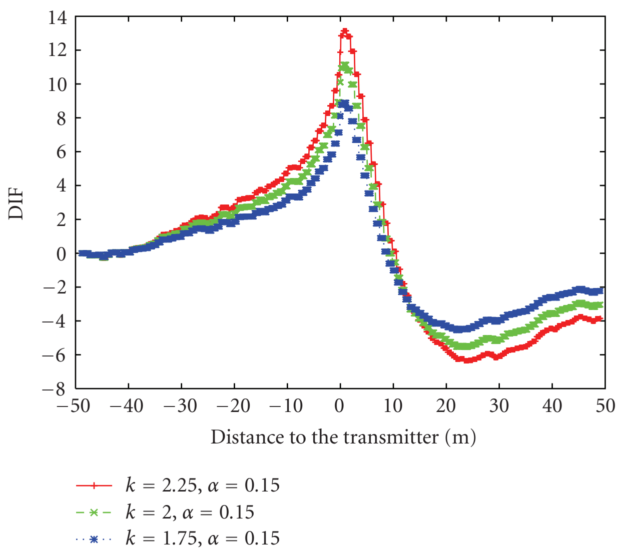

Figure 9: Effect of k in WLAN.

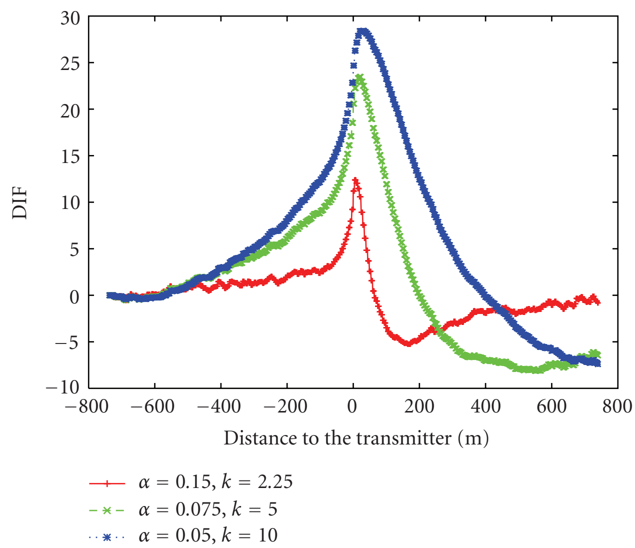

Figure 11: Effect of α and k in WMAN.

propagation, a longer distance between the user and the transmitter corresponds to a smaller rate of DIF change. When the user leaves the transmitter and the distance between the user and the transmitter exceeds a certain value, the DIF rebounds.

The results in Figures 8 and 9 indicate that a larger α and k enable rapid and accurate identification of user motion state. However, α and k are inversely related to those (α, k) pairs that minimize incorrect movement detection. Therefore, three (α, k) pairs are selected based on Figure 5 to study the UMD characteristics in WLAN and WMAN. Figure 10 presents the effect of three (α, k) pairs on the DIF value. A larger α and smaller k can cause DIF to drop quickly when the user moves away from the transmitter but causes DIF to slowly rise when the user approaches the transmitter.

In a WMAN environment, a user is moving from location A to location C at 12.5 m/sec. Figure 11 demonstrates the variation of the DIF value. If the same parameters used for WLAN ($\alpha = 0.15$, $k = 2.25$) are also used in WMAN, detecting user behavior becomes very difficult because the smaller k corresponds to a smaller ΔDIF and a larger α makes ΔDIF drops quickly as the user moves away from the transmitter in WMAN. Therefore, based on the simulation results and analysis, α and k must be smaller and larger, respectively, in a WMAN environment than in a WLAN environment.

Figure 12 illustrates the effect of shadowing deviation on the DIF value as the user moves from location A to location C at 1 m/sec in a WLAN environment. The simulation results reveal that UMD eliminates almost all RSS

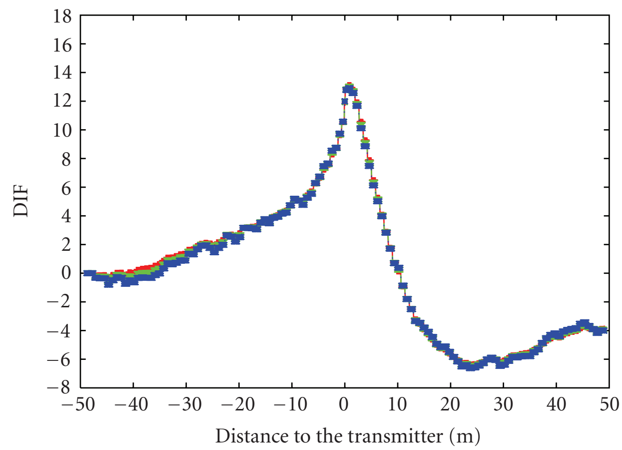

Figure 12: Effect of shadowing deviation in WLAN.

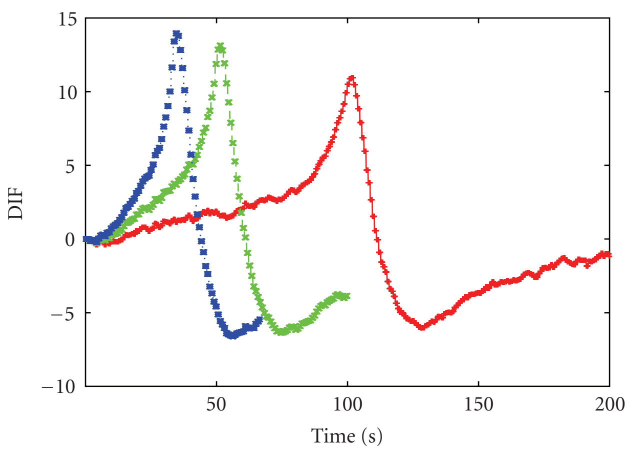

Figure 13: Effect of velocity in WLAN.

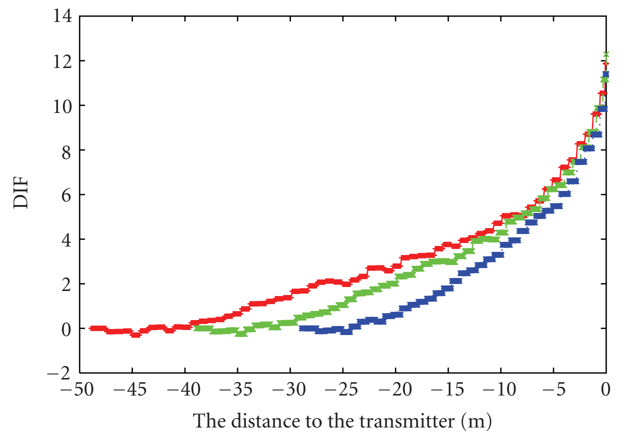

(a) The effect of DIF when an MT approaches away AP from different distance in WLAN

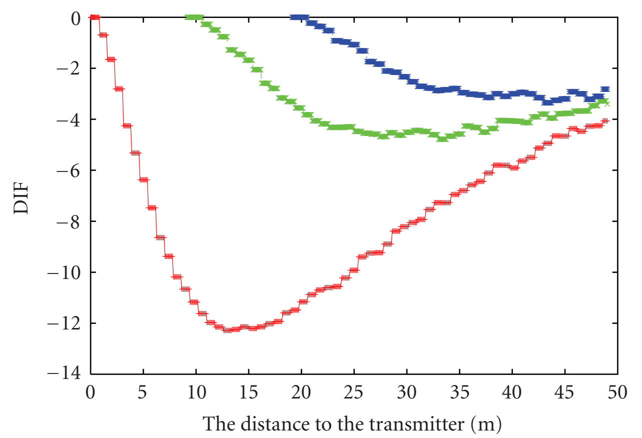

(b) The effect of DIF when an MT moves AP from different distance in WLAN

Figure 14: MT approaching and moving away AP from various distances.

fluctuations. Figure 13 shows how velocity affects the DIF value for the same movement trajectory when the user is in a WLAN environment. The results indicate that higher velocity corresponds with a greater rate of DIF change.

Figure 14 displays the effect of starting point on DIF variation as the user moves at 1 m/sec in a WLAN environment. Figure 14(a) shows that the DIF values are almost independent of starting position when the user approaches the transmitter. Figure 14(b) presents the DIF change when a user leaves from AP at various locations. The results reveal that the rate of DIF change declines as the starting position of a user is farther away from the transmitter. As Figure 14 shows, the mobile radio propagation strongly affects the behavior of UMD. As the distance between an MT and its transmitter increases, the sensitivity of UMD in motion detection with a fixed α and k declines.

4.1.2. *Feasibility of UMD mechanism*

The random waypoint mobility model is adopted to simulate a single user in a WLAN and a WMAN environment to study the feasibility of UMD. Table 2 shows the related settings of the simulation parameters.

Figure 15(a) shows the user motion trajectory in a WLAN environment. The user temporarily remains stationary at each turning point. Table 3 shows the detailed user movement data. Figure 15(b) shows the measured RSS value from the MT. Figure 16 displays the variation in the DIF value obtained by the MT, and the symbols on the x-axis indicate the locations presented in Figure 15(a). The simulation result confirms that the DIF value can easily

Table 2: Parameters for UMD mechanism and random waypoint mobility model.

	WLAN	WMAN
User velocity (m/s)	0.5–2.5	0.5–27.7
Max pause (second)	60	180
Duration (second)	400	800
α	0.15	0.075
k	2.25	5.0

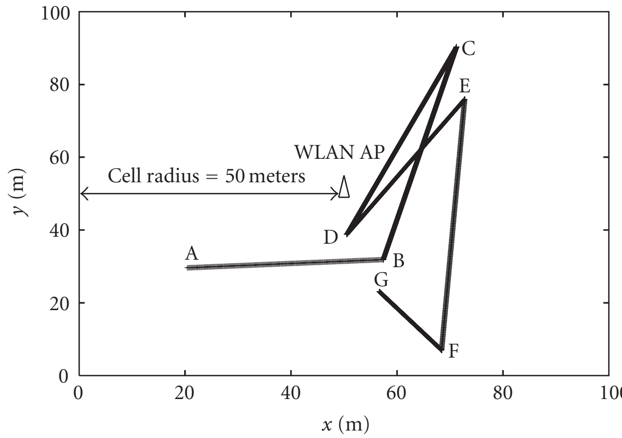

(a) The trajectory of the MT in WLAN (random waypoint model)

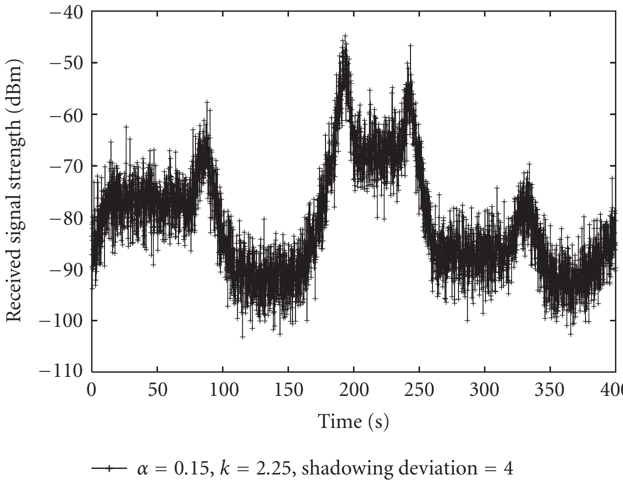

(b) Received signal strength measured by the MT in WLAN

Figure 15: User motion trajectory and the RSS measured by the MT in WLAN.

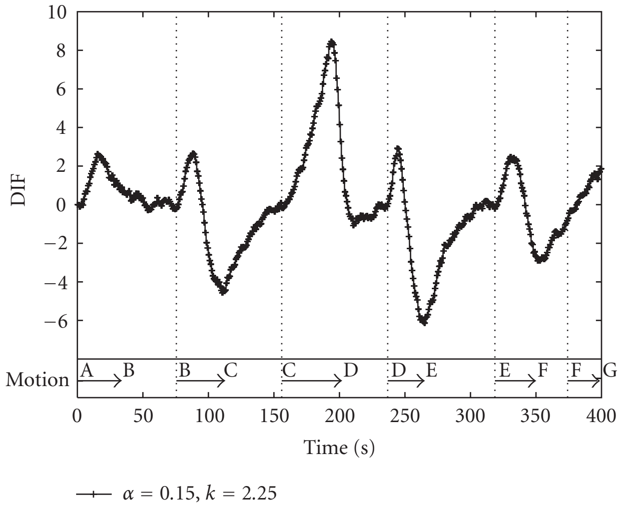

Figure 16: Variation in DIF value obtained by the MT in WLAN.

Table 3: Parameters of user motion in WLAN.

Start	End	Duration (second)	Velocity (m/s)
A	B	18.252303	2.035956
B	B	57.295744	0
B	C	35.670937	1.682126
C	C	44.752047	0
C	D	44.779019	1.239218
D	D	36.085495	0
D	E	26.587702	1.625802
E	E	55.217815	0
E	F	30.340680	2.269885
F	F	25.141795	0
F	G	25.876464	0.769553

Table 4: Parameters of user motion in WMAN.

Start	End	Duration (second)	Velocity (m/s)
A	B	66.936229	14.609059
B	B	80.483504	0
B	C	312.523963	3.495420
C	C	175.488542	0
C	D	28.918318	16.878986

determine the user motion state: stationary, leaving, and approaching—by using UMD.

Figure 17(a) shows the user motion trajectory in a WMAN environment. At each turning point, the user remains stationary for a period. Table 4 presents in detail user motion data. Figure 17(b) shows the measured RSS value from the MT in the WMAN environment. Figure 18 shows the DIF in the WMAN environment. When a small α and a large k are used in the simulation, the stationary state cannot be detected quickly (such as when the user is at location B) unless a user is stationary for a long time (such as at location C).

4.1.3. Experiment

The feasibility of UMD was investigated experimentally. A laptop with an Intel PRO/Wireless 2200BG network connection mini PCI adapter and a D-Link DWL-3200 AP were used. The authors randomly walked around the AP and continuously recorded RSS to determine the DIF value. Figure 19 plots the RSS measured by an MT over time, and Figure 20 presents the calculated DIF value. The

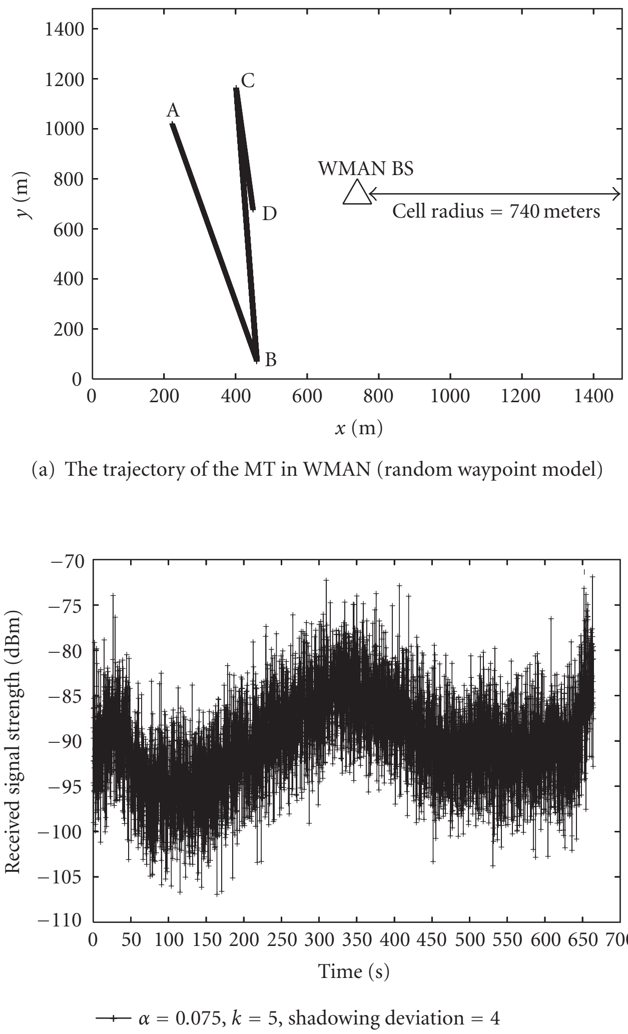

(a) The trajectory of the MT in WMAN (random waypoint model)

(b) Received signal strength measured by the MT in WMAN

Figure 17: User motion trajectory and the RSS measured by the MT in WMAN.

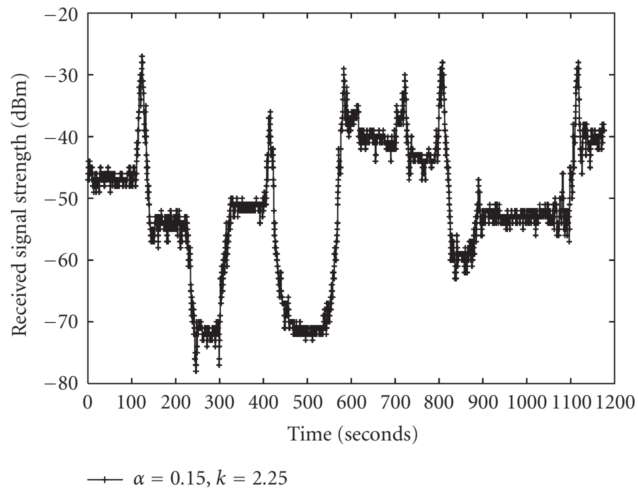

Figure 19: Measured received signal strength.

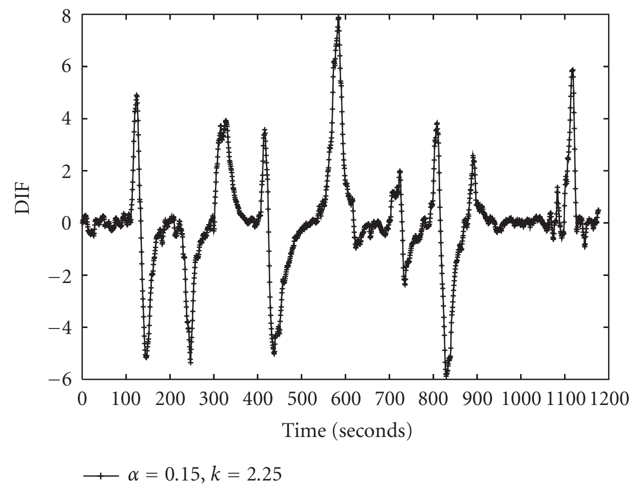

Figure 20: Variation in DIF value throughout experiment.

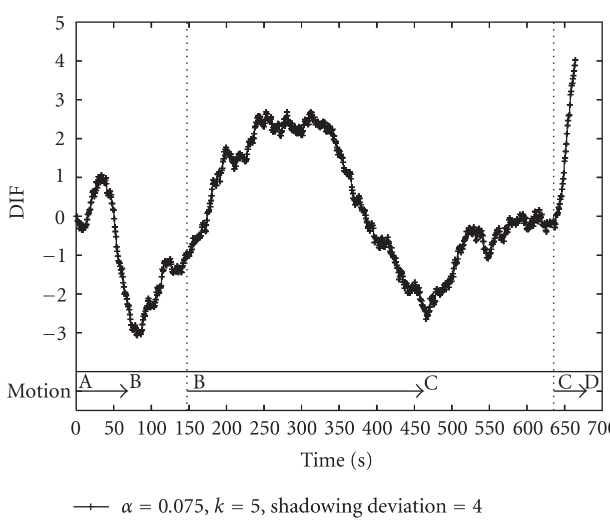

Figure 18: Variation of DIF value obtained by the MT in WMAN.

experimental results demonstrate that the proposed UMD mechanism clearly identifies the user motion state.

4.2. *Evaluation of NDMD algorithm*

The performance of NDMD was compared with RSS threshold-based handoff algorithm [15], RSS threshold combined with dwell-time-based handoff algorithms [16], RSS threshold combined with hysteresis-based handoff algorithm [16], RSS threshold combined with hysteresis and dwell-time-based handoff algorithms [16] and geographic-based handoff algorithm [12].

(i) In RSS threshold-based method, an MT initiates a network discovery to search available networks in its neighborhood when RSS of current servicing access point (RSS_{old}) is lower than a predefined network discovery threshold (TH_{ND}). Then, the MT triggers a handoff when RSS_{old} is lower than a predefined

Table 5: Default parameters in a WLAN environment for the simulation of NDMD algorithm.

Parameter	Value	Parameter	Value
Cell radius (m)	100	Tx Power (dBm)	22
Frequency (Hz)	2.472e9	Rx sensitivity (dBm)	−94
Transmitter antenna height (m)	1	Receiver antenna height (m)	1
Transmitter antenna gain (dB)	1	Receiver antenna gain (dB)	1
Path loss exponent	4.0	Sampling interval (second)	0.05
Shadowing deviation (dB)	4.0	Sampling size	8

Table 6: Parameters of random waypoint mobility model.

Velocity (m/s)	0.5–2.5
Max pause (second)	60
Duration (second)	86400
Network discovery preprocessing time	5 sec

handoff threshold (TH_{HO}) and RSS_{old} is lower than the RSS of neighborhood access point (RSS_{new}).

(ii) In RSS threshold combined with dwell-time-based handoff algorithms, an MT triggers a network discovery when $TH_{ND} > RSS_{old}$ and initiates a handoff when $TH_{HO} > RSS_{old}$ and this state is maintained over a dwell time.

(iii) In RSS threshold combined with hysteresis-based method, an MT triggers a network discovery when $TH_{ND} > RSS_{old}$ and initiates a handoff when $TH_{HO} > RSS_{old}$ and $RSS_{new} > RSS_{old} + H$, where H is a given hysteresis value.

(iv) RSS threshold combined with hysteresis and dwell-time-based handoff algorithms is a combination of above three methods.

(v) In geographic-based handoff method, an MT initiates a handoff according to a GPS and topology map information from a resource manager.

The simulations evaluated the performance of NDMD in terms of the power consumption, total number of handoff and total number of fail handoff.

(i) *Power consumption:* an accumulated all interfaces activated time in WLAN. A larger active time represents larger power consumption.

(ii) *Number of handoff:* handoff process switches the connection between different access points and may stop the transmission in a while. Thus, unnecessary handoffs may decrease the performance of a communication system.

(iii) *Number of failed handoff:* since discovering available networks requires a nonnegligible time, a handoff may fail if an MN starts network discovering late. Moreover, unnecessary handoffs may increase the risk of connection break due to handoff failure.

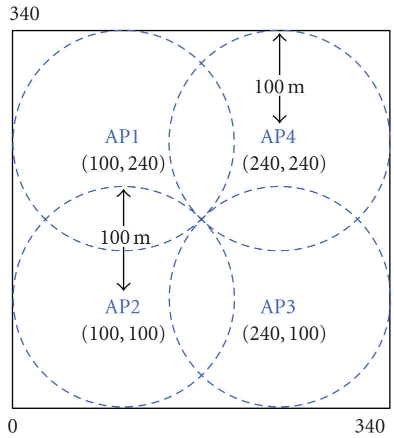

Figure 21: The deployment of overlay WLAN.

Figure 21 shows an indoor WLAN overlay structure was used to evaluate the performance of different network discovery mechanism. The authors use four adjacent cells with 100-meter radius. The BSs are located in the same floor with the following coordinates: (100, 240), (100, 100), (240, 100), and (240, 240). An MT is equipped with four network interfaces. A log normal shadowing model is used and simulation parameters for an indoor WLAN environment are set as presented in Table 5. In the simulations, the random waypoint mobility model is adopted to generate the tour of a mobile user. Table 6 presents simulation parameters for the random waypoint mobility model. Since the user is in an indoor environment, the range of velocities is set between 0.5 m/sec and 2.5 m/sec. A preprocessing time is introduced to represent the latency of the network discovery procedure including the time required to activate interface, search base station, associate with a chosen AP, and so forth. The parameters of various approaches and thresholds are presented in Table 7.

Figure 22 shows the accumulated active time of all interfaces in various approaches. In Figure 22, the RSS threshold-based method and the RSS threshold combined with dwell-time-based method consumes more power than other approaches. In the RSS threshold-based method, an MT turns on all interfaces to search available access networks and executes handoff procedure only according to TH_{ND} and TH_{HO}. In NDMD, an MT can identify the user motion state. When the MT is in a stationary state, the MT turns off other interfaces to reduce power consumption. Thus, NDMD consumes less power than other approaches. Moreover, the dwell time method requires an MT to turn on all interfaces for checking their RSS from neighborhood access points over a dwell time, thus the dwell time method consumes much power.

Figure 23 shows the accumulated number of handoff. In Figure 23, geographic-based handoff method has the lowest number of handoff because it triggers handoff process and

Table 7: Parameters for different handoff mechanisms.

Method	NDMD	NDMD	T	T	T + D	T + D	T + H + D	T + H + D	T + H	T + H	Geographic-based
α	0.15	0.15	None	None	None	None	None	None	None	None	None
k	5.5	5.5	None	None	None	None	None	None	None	None	None
TH_N (dBm)	−1	−1	None	None	None	None	None	None	None	None	None
TH_P (dBm)	1	1	None	None	None	None	None	None	None	None	None
Hysteresis (dBm)	None	None	None	None	None	None	10	10	10	10	None
TH_{ND} (dBm)	−87	−92	−87	−92	−87	−92	−87	−92	−87	−92	None
TH_{HO} (dBm)	−87	−92	−87	−92	−87	−92	−87	−92	−87	−92	None
TH_{Dwell} (sec)	None	None	None	None	4	4	4	4	None	None	None

T: Threshold/D: Dwell-time/H: Hysteresis.

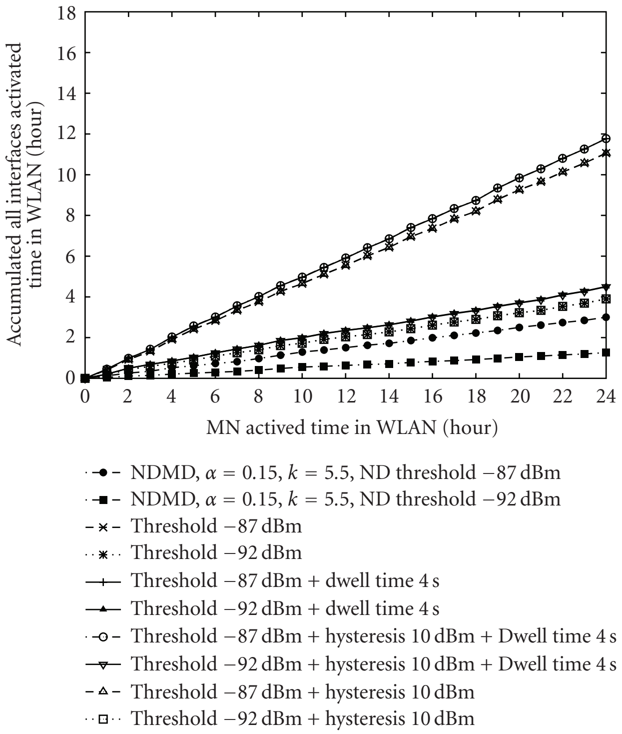

Figure 22: Accumulated active time of all interfaces in WLAN.

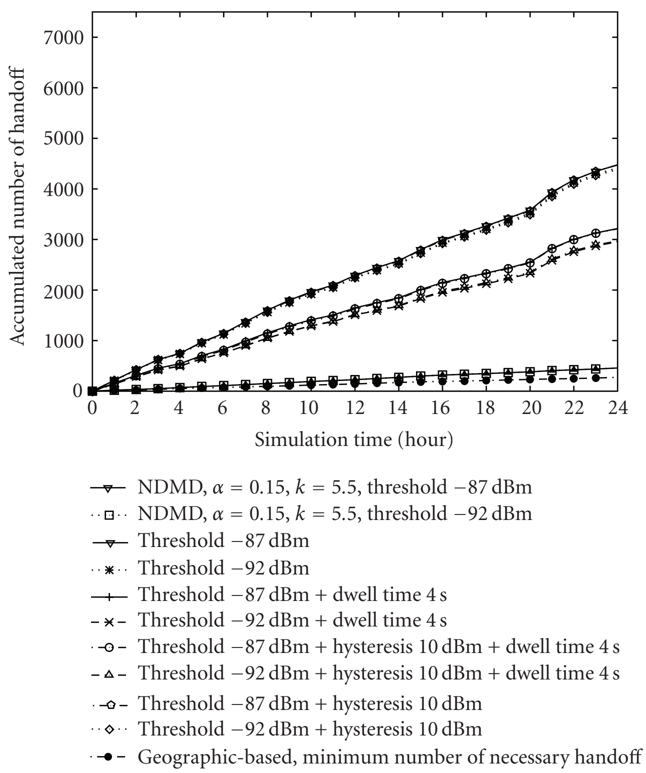

Figure 23: Accumulated number of handoff in WLAN.

switches MT's connection to a new AP according to MT's location information from a GPS and a location server (resource manager server). Since NDMD can identify user motion of an MT, NDMD can reduce unnecessary handoffs. On the other hand, the RSS threshold based algorithms has the largest number of handoff due to an MT always triggers network discovery and handoff when the MT is in a stationary state. Moreover, the dwell time method limits the handoff trigger by a time constraint during the network discovery, thus the MT triggers handoff late and reduces unnecessary handoffs. Nevertheless, both RSS threshold based method, RSS threshold combined with dwell time based method, RSS threshold combined with hysteresis based method, and RSS threshold combined with hysteresis and dwell time based method cause larger number of unnecessary handoffs. Figure 24 shows the accumulated number of failed handoff in WLAN. In Figure 24, NDMD performs better than other algorithms because NDMD can determines user motion, activates and terminates MT's interfaces rapidly enough to reduce unnecessary handoffs.

5. CONCLUSION AND FUTURE WORK

This work presents MACD-based user motion detection mechanism (UMD) and a predictive algorithm called NDMD for network discovery in heterogeneous wireless network environments. Without any assistance from a positioning system, UMD can identify the user's behavior correctly. The NDMD determines when a user leaves, approaches or remains stationary with respect to its associated access point by UMD and then initiates or terminates the corresponding

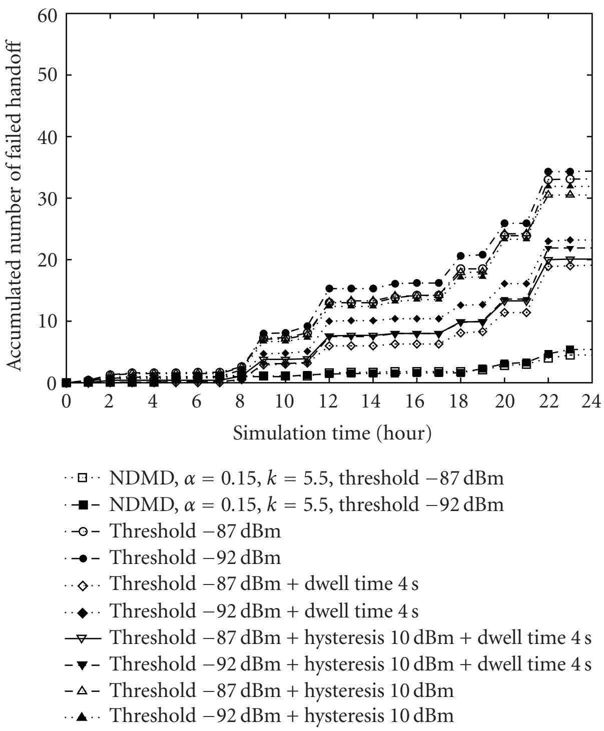

FIGURE 24: Accumulated number of failed handoff in WLAN.

network discovery procedure in an appropriate time. The simulation results demonstrate that NDMD can immediately determine when a user is leaving the coverage area of a wireless network and then activates interfaces to perform network discovery in time. Thus, the system not only reduces handoff dropping rate, it also terminates the interfaces whenever a user remains stationary or approaches the transmitter. Therefore, it can reduce the power consumption of network discovery at a mobile node. Additionally, NDMD can trigger and terminate network discovery in time, it can be easily incorporated into existing handoff decision schemes, such as dwell time approaches, hysteresis approaches, and the combination of above approaches to reduce handoff dropping rate and power consumption in handoff process.

However, some problems with the UMD mechanism remain to be solved. The mobile radio propagation features degrade the sensitivity of the UMD mechanism as the distance between an MT and its transmitter increases. The UMD mechanism must use different configurations for various wireless networks. Therefore, future work may explore the dynamic adaptation of the UMD configuration to various wireless networks.

ACKNOWLEDGMENT

This paper was sponsored in part by "Aim for the Top University Plan" of Yuan Ze University and Ministry of Education, Taiwan, and the National Science Council, Taiwan, under Contract no. NSC96-2221-E-155-033 and NSC97-2218-E-155-006.

REFERENCES

[1] V. Héctor and K. Gunnar, "Techniques to reduce IEEE 802.11b MAC layer handover time," TRITA-IMIT-LCN R 03:02, Royal Institute of Technology, Stockholm, Sweden, April 2003.

[2] M. Bernaschi, F. Cacace, and G. Iannello, "Vertical handoff performance in heterogeneous networks," in *Proceedings of the International Conference on Parallel Processing Workshops (ICPPW '04)*, pp. 100–107, Montreal, Canada, August 2004.

[3] M. Bernaschi, F. Cacace, G. Iannello, S. Za, and A. Pescapè, "Seamless internetworking of WLANs and cellular networks: architecture and performance issues in a mobile IPv6 scenario," *IEEE Wireless Communications*, vol. 12, no. 3, pp. 73–80, 2005.

[4] B. Liang, A. H. Zahran, and A. O. M. Saleh, "Application signal threshold adaptation for vertical handoff in heterogeneous wireless networks," in *Proceedings of the 4th International IFIP-TC6 Networking Conference (NETWORKING '05)*, vol. 3462 of *Lecture Notes in Computer Science*, pp. 1193–1205, Waterloo, Canada, May 2005.

[5] H. S. Park, S. H. Yoon, T. H. Kim, J. S. Park, M. S. Do, and J. Y. Lee, "Vertical handoff procedure and algorithm between IEEE802.11 WLAN and CDMA cellular network," in *Proceedings of the 7th CDMA International Conference on Mobile Communications (CIC '02)*, vol. 2524 of *Lecture Notes in Computer Science*, pp. 103–112, Seoul, Korea, October-November 2002.

[6] C. W. Lee, L. M. Chen, M. C. Chen, and Y. S. Sun, "A framework of handoffs in wireless overlay networks based on mobile IPv6," *IEEE Journal on Selected Areas in Communications*, vol. 23, no. 11, pp. 2118–2128, 2005.

[7] W.-T. Chen and Y.-Y. Shu, "Active application oriented vertical handoff in next-generation wireless networks," in *Proceedings of IEEE Wireless Communications and Networking Conference (WCNC '05)*, vol. 3, pp. 1383–1388, New Orleans, La, USA, March 2005.

[8] G. Appel, *The Moving Average Convergence-Divergence Trading Method*, Traders Press, Toronto, Canada, 1985.

[9] M. Ylianttila, J. Mákelá, and K. Pahlavan, "Analysis of handoff in a location-aware vertical multi-access network," *Computer Networks*, vol. 47, no. 2, pp. 185–201, 2005.

[10] P. Khadivi, T. D. Todd, and D. Zhao, "Handoff trigger nodes for hybrid IEEE 802.11 WLAN/cellular networks," in *Proceedings of the 1st International Conference on Quality of Service in Heterogeneous Wired/Wireless Networks (QSHINE '04)*, pp. 164–170, Dallas, Tex, USA, October 2004.

[11] W.-T. Chen, J.-C. Liu, and H.-K. Huang, "An adaptive scheme for vertical handoff in wireless overlay networks," in *Proceedings of the 10th International Conference on Parallel and Distributed Systems (ICPADS '04)*, pp. 541–548, Newport Beach, Calif, USA, July 2004.

[12] M. Inoue, G. Wu, K. Mahmud, H. Murakami, and M. Hasegawa, "Development of MIRAI system for heterogeneous wireless networks," in *Proceedings of the 13th IEEE International Symposium on Personal, Indoor and Mobile Radio Communications (PIMRC '02)*, vol. 1, pp. 69–73, Lisbon, Portugal, September 2002.

[13] A. Sur and D. C. Sicker, "Multi layer rules based framework for vertical handoff," in *Proceedings of the 2nd International Conference on Broadband Networks (BROADNETS '05)*, vol. 1, pp. 571–580, Boston, Mass, USA, October 2005.

[14] J. Hightower and G. Borriello, "Location systems for ubiquitous computing," *Computer*, vol. 34, no. 8, pp. 57–66, 2001.

[15] ETSI, GSM Technical Specification, GSM 08.08, version 5.12.0 ed., France, June 2000.

[16] S. Shirvani Moghaddam, V. Tabataba Vakili, and A. Falahati, "New handoff initiation algorithm (optimum combination of hysteresis and threshold based methods)," in *Proceedings of the 52nd IEEE Vehicular Technology Conference (VTC '00)*, vol. 4, pp. 1567–1574, Boston, Mass, USA, September 2000.

[17] J. McNair and F. Zhu, "Vertical handoffs in fourth-generation multinetwork environments," *IEEE Wireless Communications*, vol. 11, no. 3, pp. 8–15, 2004.

[18] F. Zhu and J. McNair, "Optimizations for vertical handoff decision algorithms," in *Proceedings of IEEE Wireless Communications and Networking Conference (WCNC '04)*, vol. 2, pp. 867–872, Atlanta, Ga, USA, March 2004.

[19] A. Hasswa, N. Nasser, and H. Hassanein, "Generic vertical handoff decision function for heterogeneous wireless networks," in *Proceedings of International Conference on Wireless and Optical Communications Networks (WOCN '05)*, pp. 239–243, Dubai, United Arab Emirates, March 2005.

[20] T. Al-Gizawi, K. Peppas, D. I. Axiotis, E. N. Protonotarios, and F. Lazarakis, "Interoperability criteria, mechanisms, and evaluation of system performance for transparently interoperating WLAN and UMTS-HSDPA networks," *IEEE Network*, vol. 19, no. 4, pp. 66–72, 2005.

[21] The Network Simulator - ns-2, http://www.isi.edu/nsnam/ns/.

[22] "BonnMotion: a mobility scenario generation and analysis tool," http://web.informatik.uni-bonn.de/IV/Mitarbeiter/dewaal/BonnMotion/.

[23] X. Wu and A. L. Ananda, "Link characteristics estimation for IEEE 802.11 DCF based WLAN," in *Proceedings of the 29th Annual IEEE International Conference on Local Computer Networks (LCN '04)*, pp. 302–309, Tampa, Fla, USA, November 2004.

[24] Airspan Corporation, http://www.airspan.com/.